Eur. Phys. J. B **45**, 317–324 (2005)
DOI: 10.1140/epjb/e2005-00203-7

THE EUROPEAN PHYSICAL JOURNAL B

Optical characterization of the polymer embedded alloyed bimetallic nanoparticles

V.I. Belotelov[1], G. Carotenuto[2], L. Nicolais[2], G.P. Pepe[3,a], and A.K. Zvezdin[4]

[1] M.V. Lomonosov Moscow State University, Faculty of Physics, 119992, Leninskie gori, Moscow, Russia
[2] Italian National Research Council, Naples, 80125, P.le Tecchio 80, Naples, Italy
[3] Università di Napoli "Federico II", Dip. Scienze Fisiche, 80125, P.le Tecchio 80, Naples, Italy
[4] General Physics Institute, RAS, 119991, Vavilov St., 38, Moscow, Russia

Received 9 March 2005 / Received in final form 11 April 2005
Published online 6 July 2005 – © EDP Sciences, Società Italiana di Fisica, Springer-Verlag 2005

Abstract. A theoretical approach for the calculation of the bimetallic nanoparticles absorption spectra has been developed as an extension of the Mie theory in which nanoparticle dielectric function is found by the weighted linear combination of the dielectric functions for particles made of the corresponding pure metals. In the frame work of the theoretical model an expression for the resonance light absorption frequency were derived taking into account the interband transitions in the dielectric functions. We propose a simple method for the on-line monitoring of the bimetallic nanoparticles composition based on the measurement of the absorption peak position. Elaborated theoretical approach was used to investigate the polymer embedded Ag/Au nanoparticles which were prepared by reducing gold and silver salts (HAuCl4 and AgNO3, respectively) by ethylene glycol in presence of poly(vinyl pyrrolidone) (PVP) at room temperature. Calculated absorption spectra for the Ag/Au nanoscopic systems showed good agreement with the experimental data. Temporal evolution of the Ag/Au nanoparticles has also been investigated by this approach.

PACS. 78.66.Bz Metals and metallic alloys – 78.67.Bf Nanocrystals and nanoparticles – 73.20.Mf Collective excitations (including excitons, polarons, plasmons and other charge-density excitations)

1 Introduction

Recently, there has been much attention paid to the creation and investigation of bimetallic alloyed nanoparticles owing to their interesting surface plasma band energy [1–3], catalytic [4], non-linear optical properties, especially THG (third harmonic generation), and magnetic properties [5,6], which are different from the ones of the individual metals. The magnetic properties of colloidal ferromagnetic nanoparticles have been studied for their application to ferrofluids [7–9]. Bimetallic nanoclusters can also be widely exploited for use in biological labeling, surface enhanced Raman scattering (SERS), etc. [10]. The intense research in this field is also motivated by the search for new multifunctional materials that will allow designing of the modern miniature electronic and optical devices for ultra fast data communication and optical data storage. Nanoelectronic devices prepared from careful construction of two- or three-dimensional layers of bimetallic nanoparticles are now a hot topic.

Among different types of the bimetallic alloys Ag/Au nano-systems receive the most significant attention because of their unique optical and electrochemical properties [2,3,11,12].

The intrinsic properties of a nano-structured metal are mainly determined by its size, shape, composition, crystallinity, and structure. In principle, accurate control of any one of these parameters allows for fine tuning of the properties of nano-structured material-based devices.

One of the main metallic nanoclusters optical features is that they have broad absorption band in the visible region of the electromagnetic spectrum [13]. Fluid and polymer systems of the noble metals copper, gold, and silver show a very intense colors, which are absent for the bulk materials. Their origin is attributed to the surface plasmons – collective oscillation of the free conduction electrons induced by the incident electromagnetic radiation. The frequency position of the surface plasmon resonance in the alloyed nanoclusters is strongly dependent on the alloy composition and can be tuned finely by the composition appropriate choice [2]. The latter is of prime importance in connection to the possible applications for the light-stable color filters [14], polarizers [15], optical sensors [16], etc.

Several methods have been used to prepare bimetallic nanoparticles, including radiolytic [17], alcohol [18], citrate [12], photolytic [19], and borohydride [20] reduction,

[a] e-mail: gpepe@na.infn.it

metal evaporation-condensation [21], and sonochemical methods [22]. The particles diameters were usually constrained by protective agents such as soluble polymers and organic ligands.

The embedding of nanosized metal structures into polymeric matrices represents the most simple way to protect clusters and to take advantage of their physical characteristics [23]. Polymer matrices provide opportunity for the nanocomposites to have tunable optical properties under influence of mechanical stresses or at temperature changes [24]. That is why their use for nanocomposites host media is of the great interest.

Polymer-embedded alloyed clusters can be obtained by using two different approaches, which can be classified as in situ and ex situ. In the in situ methods, metal clusters are generated inside a polymer matrix by decomposition or chemical reduction of a metallic precursor dissolved into the polymer. In the ex situ approach, clusters are first produced by soft-chemistry routes and then dispersed into polymeric matrices.

Since the performance of a nanostructured material depends on its physical properties, which are related to a variety of structural factors (size, shape or composition), on-line in situ morphological monitoring techniques play a role of primary importance. Since metallic nanoparticles demonstrate pronounced absorption peaks in their UV-Vis-NIR spectra which are strongly influenced by the nanoparticles composition the use of real-time optical spectroscopy is an efficient in situ monitoring method [25]. In particular, the position of the surface plasmonic resonance depends on the alloyed nanoparticle relative content and can be utilized to determine it.

Strong optical resonance absorption of light is due to collective excitations of the quasifree electrons known as surface plasmon polariton or particle plasmon resonance [26]. Plasmon resonances can be described either by the classical electrodynamics methods [27] or, on the microscopic level in the density functional theory [28]. The latter, though being quite exact due to its self-consistent ab initio basis, faces many computation constraints when applied to description of large clusters, so electrodynamic Mie theory approach is widely used. It works properly for nanoclusters of sizes more than several nanometers where the quantum-size effects are negligible. Electromagnetic radiation absorption by tiny particles of pure metals has been studied extensively by many authors [13,25,26,29]. At the same time, bimetallic alloyed nanoparticles were considered only in a few works [1–3]. Calculation of the plasmon resonance in the alloyed nanoclusters, being very important task, is not trivial. Dielectric function of the alloyed system should be chosen appropriately, the interband transitions being also taken into account.

This article is addressed to the problem of the light absorption by polymer embedded alloyed metallic nanoparticles, which includes conduction of the theoretical analysis and corresponding experimental investigation. In Section 2 we develop a theoretical approach for the calculation of the bimetallic alloyed nanoclusters absorption spectra. Section 3 describes polymer nanocomposite preparation procedure and experimental setup. Section 4 is a results and discussion part in which theoretical and experimental data are compared and the possibility for the determination of the alloyed nanoparticles relative content via their absorption spectra is investigated.

2 Theoretical analysis

When electromagnetic radiation interacts to the nanoparticles medium absorption and scattering processes arise which results in directly transmitted light intensity got smaller than the incident intensity by a factor of $\exp(n\sigma_{ext}l)$, where n – concentration of nanoparticles in the composite, σ_{ext} is the extinction cross section, end l is the sample's thickness. For the metallic particles of the size less than 50 nm the absorption efficiency is much higher than the scattering one, so in the literature the term "absorption" is usually used to substitute the term "extinction". At the experimental spectroscopy it is absorbance A that is measured actually. The absorbance A is related to the extinction cross section by $A = n\sigma_{ext}l \log 10$.

That is why to approximate experimental data with some theoretical curves one need to calculate the extinction cross section. In the presence of the dilute colloidal solution for which nanoparticles take a solution volume fraction f less than 0.01 it is possible to neglect all interparticle interactions and regard the composite extinction cross section being proportional to the one for single particle. An additional assumption concerning spherical form of the particle leads to the Mie scattering theory. This theory provides an exact analytical electrodynamical treatment for the light of wavelength λ scattering and absorption by the uncharged spherical particle of radius r with dielectric function ε in a homogeneous medium of the dielectric function ε_m [27,30]. In the Mie theory, the extinction cross section is calculated by:

$$\sigma_{ext} = 2\pi/(\varepsilon_m k_0^2) \sum_{n=1}^{\infty} (2n+1)\mathrm{Re}(a_n + b_n), \qquad (1)$$

where $k_0 = 2\pi/\lambda$, a_n and b_n are the Mie coefficients which are

$$a_n = \frac{m\psi_n(mx)\psi_n'(x) - \psi_n(x)\psi_n'(mx)}{m\psi_n(mx)\xi_n'(x) - \xi_n(x)\psi_n'(mx)}, \qquad (2)$$
$$b_n = \frac{\psi_n(mx)\psi_n'(x) - m\psi_n(x)\psi_n'(mx)}{\psi_n(mx)\xi_n'(x) - m\xi_n(x)\psi_n'(mx)},$$

with $m = \sqrt{\varepsilon/\varepsilon_m}$, $x = \sqrt{\varepsilon_m}k_0 r$, and the Riccati-Bessel functions ψ_n and ξ_n [27].

Expressions (2) can be expanded into series on parameter x leading to the

$$a_1 = -\frac{2}{3} i \varepsilon_m^{3/2} \frac{\varepsilon - \varepsilon_m}{\varepsilon + 2\varepsilon_m} x^3 + O(x^5), \qquad (3)$$
$$b_1 = O(x^5), a_2 = O(x^5), \text{ and so on.}$$

If the particle is much smaller compared to the light wavelength only the first electric dipole term, i.e. Re (a_1) in (1)

can be left. Such approximation remains valid for particle's diameter smaller than 15–20 nm, which is the case of our current work. That is why at the processing of experimental data we used the following extinction cross section

$$\sigma_{ext} = \frac{\lambda^2}{\pi} \frac{\varepsilon_2}{(\varepsilon_1 + 2\varepsilon_m)^2 + \varepsilon_2^2} x^3, \quad (4)$$

where $\varepsilon = \varepsilon_1 + i\varepsilon_2$.

This expression can also be obtained by purely electrostatic approach, neglecting effects due to self-induction of electromagnetic fields (retardation) [31].

In this work we shall treat nanoparticles as the perfect spheres which is justified by the TEM images of the samples. At the same time, the situation when the nanoparticles shapes differ from spherical ones is quite often. In this case the expressions for the Mie coefficients get cumbersome. Nevertheless, it by no means limits the theoretical consideration, but only makes it more complex. The formulae for the Mie coefficients of the ellipsoids, cylinders, and some other shapes can be found elsewhere [26], and can be readily utilized in the theory presented further.

In order to use formula (4) it is vital to know nanoparticle dielectric function ε which differs from the one for the bulk medium. However, it is generally accepted that a good approximation to the dielectric function of small particles is easily obtained from the bulk dielectric function [32]. Indeed, if the size of the particle is not less than several nanometers then all quantum effects can be neglected and the only point to be introduced is the conduction electrons scattering on the particles surfaces. While dealing with nanoparticles of the radii in the range of 5–20 nm this surface scattering is the main reason for nanoparticles dielectric function being dependent on their sizes. Consequently, to calculate dielectric function of the nanoparticle it is possible to utilize the one for the bulk medium but taking into account surface scattering process.

Silver and gold are not purely free electron metals and interband contribution into their dielectric function is important especially for wavelength less than 320 nm for silver and 520 nm for gold that are the boundary interband wavelengths. Consequently, their dielectric function is written by

$$\varepsilon = \varepsilon_1 + i\varepsilon_2, \varepsilon_{1,2} = \varepsilon_{1,2}^D + \chi_{1,2}^{IB},$$

$$\varepsilon_1^D = 1 - \omega_p^2/(\omega^2 + \gamma^2), \varepsilon_2^D = \omega_p^2\gamma/\Big[\omega(\omega^2 + \gamma^2)\Big], \quad (5)$$

where $\varepsilon_{1,2}^D$, $\chi_{1,2}^{IB}$ are real and imaginary parts of the free electron or Drude and interband contributions into ε, $\omega_p = \sqrt{ne^2/m^*\varepsilon_0}$ - plasma frequency, n-electron density, m^* electron effective mass, ε_0 - vacuum permittivity, γ - is the rate of electron collisions.

To account the size effects, one assumes that the mean-free path of the free electrons is limited by the particle dimensions and, consequently, as the size of the particle reduces, the rate of scattering from the particle surface γ_s begins to greatly exceed the bulk scattering rate γ_0 [33]. Surface scattering rate can be expressed in terms of the Fermi velocity V_F and particle radius R

$$\gamma_s = \frac{gV_F}{R}. \quad (6)$$

Consequently, the rate of electron collisions γ is

$$\gamma = \gamma_0 + \frac{gV_F}{R}. \quad (7)$$

For gold and silver Fermi velocity get almost the same value $V_F = 1.4 \times 10^6$ m/s [34]. Coefficient g in (6) is close to unity [26]. Actually, in many works this proportionality coefficient is used to take into consideration some other factors: electron density at the surface, anisotropy of particle, quantum mechanical computations, and effects of the interface, so its value varies from 0.1 to 3. For the subject of our study the latter factor (i.e. effects on the interface) seems to be important. Indeed, because of the preparation procedure the damping rate γ_s should be influenced by physisorption at the particle surface, which induces changes of the charge density profile normal to the particle surface [13]. For example, as it follows from the fitting experimental data with theoretical predictions for the investigated nanocomposites, the influence of physisorption leads to $g = 1.8$ for silver and $g = 1.4$ for gold.

If the size of the nanoparticle is smaller than several nanometers then quantum mechanics size effects start to play a significant role [13]. For such small objects dielectric function must be calculated using some special approaches, e.g. Kubo's quantum mechanical correction to the relaxation time [35]. In this work we have neglected any quantum mechanics effects due to the sizes of the nanoclusters exceeded 3–5 nm. Nevertheless, our approach, that is present in the article, can be adapted even for ultra small particles by incorporating aforementioned theories.

Thus, in the framework of the utilized approach all the difference between the dielectric functions for nanoclusters and bulk media are enclosed inside the free electron or Drude part of the dielectric function. The contribution due to interband transitions is believed to remain unchanged.

At the present calculations interband dielectric functions were found on the basis of the publication by Quinten [36]. Interband contribution was extracted from the full dielectric functions for the gold and silver nanoparticles of diameters of 12.6 nm and 16.6 nm, respectively, presented in [36]. Real and imaginary parts of the interband dielectric functions are shown at Figure 1.

For the pure free electron matter dielectric function is given by (5) and, as it follows from (4), the plasmonic resonance takes place at frequency

$$\Omega = \frac{\omega_p}{\sqrt{1 + 2\varepsilon_m}}. \quad (8)$$

If the influence of the interband transitions is no longer negligible then to find a maximum value for the absorption the interband dielectric function should be taken into account. However, in this case no simple formulae similar

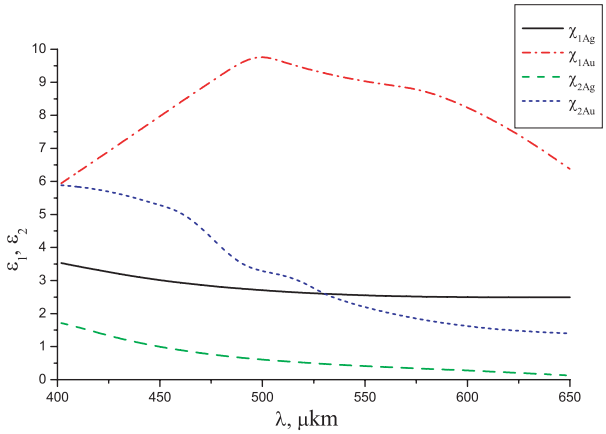

Fig. 1. Real χ_1 and imaginary χ_2 components of the interband part of the dielectric functions for silver and gold nanoparticles of the size of 12 nm and 16 nm, respectively, extracted from the Quinten data [37]. For silver: χ_1 – solid line, χ_2 – dashed line; for gold: χ_1 – dot dashed line, χ_2 – short dashed line.

to that for free electrons exist and analytical analysis of the resonance conditions gets very difficult. Sometimes it is possible to approximate the real interband part of the dielectric function by the appropriate constant value. Under additional condition that $\chi_2^{IB} \ll \chi_1^{IB}$ the following expression for the resonance frequency can be obtained from (4) and (5):

$$\Omega_1 = \frac{\omega_p}{\sqrt{1+\chi_1^{IB}+2\varepsilon_m}}. \tag{9}$$

Though, as it will be demonstrated further, equation (9) is able to determine resonance condition with good accuracy, it can only be used to estimate plasmonic frequency. Apart from that, resonance maximum width and spectra shape are also very important. Consequently, Mie theory based numerical simulations of the absorption spectra are inevitable for full optical characterization of the nanoparticles.

While dealing with the description of the optical properties of metal alloyed particles in the framework of Mie theory the most important aspect is the correct choice of the alloyed nanoparticle dielectric function. This dielectric function can be calculated in terms of dielectric functions for nanoparticles made of pure metals.

Let us consider a nanoparticle made of two metals, which we denote as metal-A and metal-B. The most straightforward matter is to assume that the dielectric function of the particle is a linear combination of the dielectric functions ε_A and ε_B for the nanoparticles of the same size but made of the pure metals "A" and "B", respectively:

$$\varepsilon = \alpha\varepsilon_A + (1-\alpha)\varepsilon_B, \tag{10}$$

where α is the relative volume concentration of the metal "A" inside the cluster. The dielectric functions ε_A and ε_B can be calculated by equations (5) and (7). As it was discussed before, information about the interband parts of the dielectric functions in (5) is readily extracted from the corresponding bulk metal dielectric functions.

Though, in some recent publications the possibility for calculation of alloyed nanoparticle dielectric function as a linear combination (10) has been argued [12], we think that this approach is acceptable and gives quite accurate results. This assertion is justified by the following.

The free electron part of dielectric function depends on the square of the plasma frequency ω_p^2. For many cases the rates of electrons collisions γ are almost the same for both metals inside the compound, consequently, the free electron parts of the dielectric functions for two metals differ only because of the ω_p^2 which is proportional to the free electron density n. At the same time, the free electron density of the alloyed nanoparticle is $n = \alpha n_A + (1-\alpha)n_B$ leading to $\varepsilon^D = \alpha\varepsilon_A^D + (1-\alpha)\varepsilon_B^D$.

However, silver and gold have close bulk plasma frequencies: $\omega_p = 8.5$ eV for silver and $\omega_p = 9.0$ eV for gold [37], and the main difference in their optical response at the visible frequency range is due to the interband transitions from the filled d bands into the sp conduction bands. At the first approximation for the case of gold and silver metals it is possible to neglect any perturbations of d-band energy levels occurring while alloying process and calculate the interband part of the dielectric function again as a linear superposition of the ones for pure metals.

Absorption spectra of the alloyed particles are very important for their characterization and also for their possible applications. Determination of the absorption spectra resonance frequency versus relative concentration of metals inside nanoparticles is of prime significance, because it enables on-line optical monitoring of nanostructures formation and allows tuning nanocomposite material exactly at desired frequency range. So far the following theoretical equation for the resonance condition in alloyed systems has been used:

$$\lambda_{bm} = \left[\alpha/\lambda_A^2 + (1-\alpha)/\lambda_B^2\right]^{-1/2}, \tag{11}$$

where λ_A and λ_B are the maximum wavelength for metals "A" and "B" respectively [38]. This equation follows from equations (9) and (10) under the condition that interband parts of dielectric functions for both metals are equal. But in reality such assumption is not valid. For example, in the wavelength range from 400 nm to 550 nm the real part of the interband dielectric functions for silver and gold can be approximated by the following constant values: $\chi_{Ag,1}^{IB} = 2.9$, $\chi_{Au,1}^{IB} = 8.5$. Taking into account this difference leads to

$$\lambda_{bm}^* = \left[\frac{\alpha(1+\chi_{A,1}^{IB}+2\varepsilon_m)\lambda_A^{-2}+(1-\alpha)(1+\chi_{B,1}^{IB}+2\varepsilon_m)\lambda_B^{-2}}{1+\alpha\chi_{A,1}^{IB}+(1-\alpha)\chi_{B,1}^{IB}+2\varepsilon_m}\right]^{-1/2}. \tag{12}$$

It is easy to see that equation (12) reduces to the conventional equation (11) if $\chi_{A,1}^{IB} = \chi_{B,1}^{IB}$.

3 Experiment

Alloyed Au-Ag clusters have been obtained by alcoholic reduction of metal salts ($HAuCl_4$, and $AgNO_3$, Aldrich).

In particular, gold and silver ions were simultaneously reduced by ethylene glycol in presence of poly(vinyl pyrrolidone) (Aldrich, Mw=10,000) as sterical stabilizer to produce alloyed bimetallic nanoparticles. The reaction was carried out at a temperature of 30 °C for a time period of 60 min. The reactive mixture contained the 25% by weight of PVP and the following gold percentages: 0.047; 0.092; 0.140; 0.183; 0.298. Since Au^{3+} and Ag^{+} ions have similar atomic radius and crystal structure (cubic face centered), Au-Ag solid solutions were obtained in the full composition range simply by modifying the quantities of two ionic precursors. Since the reduction of gold ions by ethylene glycol in presence of PVP has an induction time (due to the initial reduction of Au^{3+} to Au^{+}), typically the reaction was done by mixing a solution of $HAuCl_4$ and PVP in ethylene glycol with a freshly prepared silver solution in ethylene glycol. Since silver require the presence of PVP for reduction, the silver reduction-precipitation process starts just after mixing of two solutions. Cluster growth was ended by addition of acetone to the reactive mixture, and the isolated PVP-embedded Au-Ag clusters were dissolved in the alcoholic solution of thiol (e.g., dodecanethiol/ethyl alcohol). Dodecane thiol-derived Au-Ag clusters is a stable hydrophobic product that can be easily isolated and purified from the reactive mixture and stored for months without degradation.

The formation-growth process of gold clusters in the reactive liquid mixture was monitored by UV-Visible spectroscopy, looking at the very intensive surface plasmon absorption resonance that characterized the nano-sized metallic phase. Absorption spectra were obtained under isothermal condition at stepped reaction times by using a diode-array UV-Visible spectrophotometer (HP-8453 UV-Vis spectrophotometer), equipped with a Peltier apparatus to control the reaction temperature (from 0 to 100 °C with accuracy of ±0.1°C). The system employed a magnetic stirrer and far-UV quartz cuvettes. Absorption spectra were monitored and recorded on a personal computer connected to the spectrophotometer.

4 Results and discussion

On the basis of the developed theoretical model absorption spectra of the polymer composites with bimetallic alloyed nanoparticles of different metals content can be calculated and compared to the experimental data. This comparison can give some important information about the alloyed systems. For example, from the theoretical consideration one can determine relative metals concentration in the nanoparticles which can not be measured directly. The first approach to the solution of the problem is to calculate a set of absorption spectra for several different values of metals relative concentration and to match these spectra to the experimental ones. Such method though its sufficiently exactness is quite cumbersome. The second approach is to use equation (12) and solve it with respect to the relative concentration α. The latter is quite simple, however gives not very accurate results.

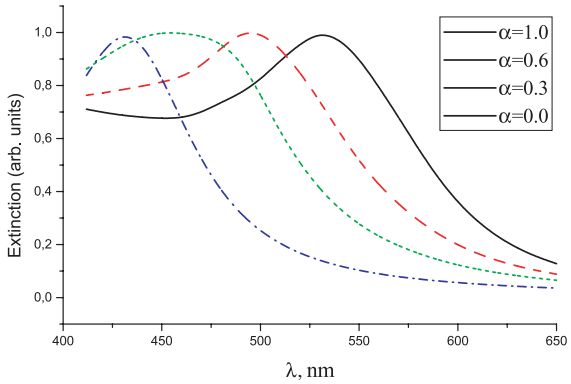

Fig. 2. Simulated absorption spectra of the Ag/Au nanoclusters inside an ethylene-glycol and PVP combined polymer matrix for the gold relative composition of (1) 0; (2) 0.3; (3) 0.6; (4) 1.0. Dielectric constant for the polymer matrix $\varepsilon_m = 2.11$ [39]; rates of electron collisions for silver and gold are $\gamma_{\mathrm{Ag}} = 5 \times 10^{13}$ s^{-1}, $\gamma_{\mathrm{Au}} = 4 \times 10^{13}$ s^{-1}; silver and gold bulk plasma frequencies: $\omega_{p(\mathrm{Ag})} = 8.5$ eV and $\omega_{p(\mathrm{Au})} = 8.5$ eV.

As an example, let us consider the Ag/Au nanoparticles polymer composite. In Figure 2 calculated absorption spectra for four different gold relative contents α are presented. The spectra maxima are normalized to unity. It can be seen that as the gold concentration increases there is a resonance peak red shift. This effect is quite expectable because plasmonic resonance for pure gold particles inside the ethylene-glycol-PVP polymer matrix takes place at the wavelength of 530 nm while the resonance for pure silver particle occurs at the wavelength of 430 nm.

In Figure 3 four experimental curves obtained in the setup described in the experimental section along with the corresponding calculated ones are presented. While the approximation of the experimental data with the calculated spectra the gold relative concentration α was considered as a fitting parameter. It should be noticed that in experiments the alloy formation was concluded from the fact that the optical absorption spectra show only one plasmon band. Two bands would be expected for the case of a mixture of separate gold and silver particles.

From Figure 3 one can conclude that the agreement between theory and experiment is quite good, except, perhaps, Figure 3b. The difference in spectra shape is due to the not exact values of the interband dielectric functions used into the calculations. Indeed, as it was mentioned before, interband dielectric functions for the nanoparticles made of pure metals were taken not directly from the experimental data but they were calculated from the experimental data in [37] for particles of different size enclosed in the different dielectric surroundings. The second reason for the deviations in spectra shapes can be related to the assumption that interband dielectric function for the alloyed systems is the linear combination of the one for pure metals disregarding *d*-band perturbation caused at alloying.

In our calculations we assumed a spherical nanoparticles shape that is justified by the TEM images. Additional confirmation for the justice of the made assertion come from the absorption spectra. Indeed, if considered

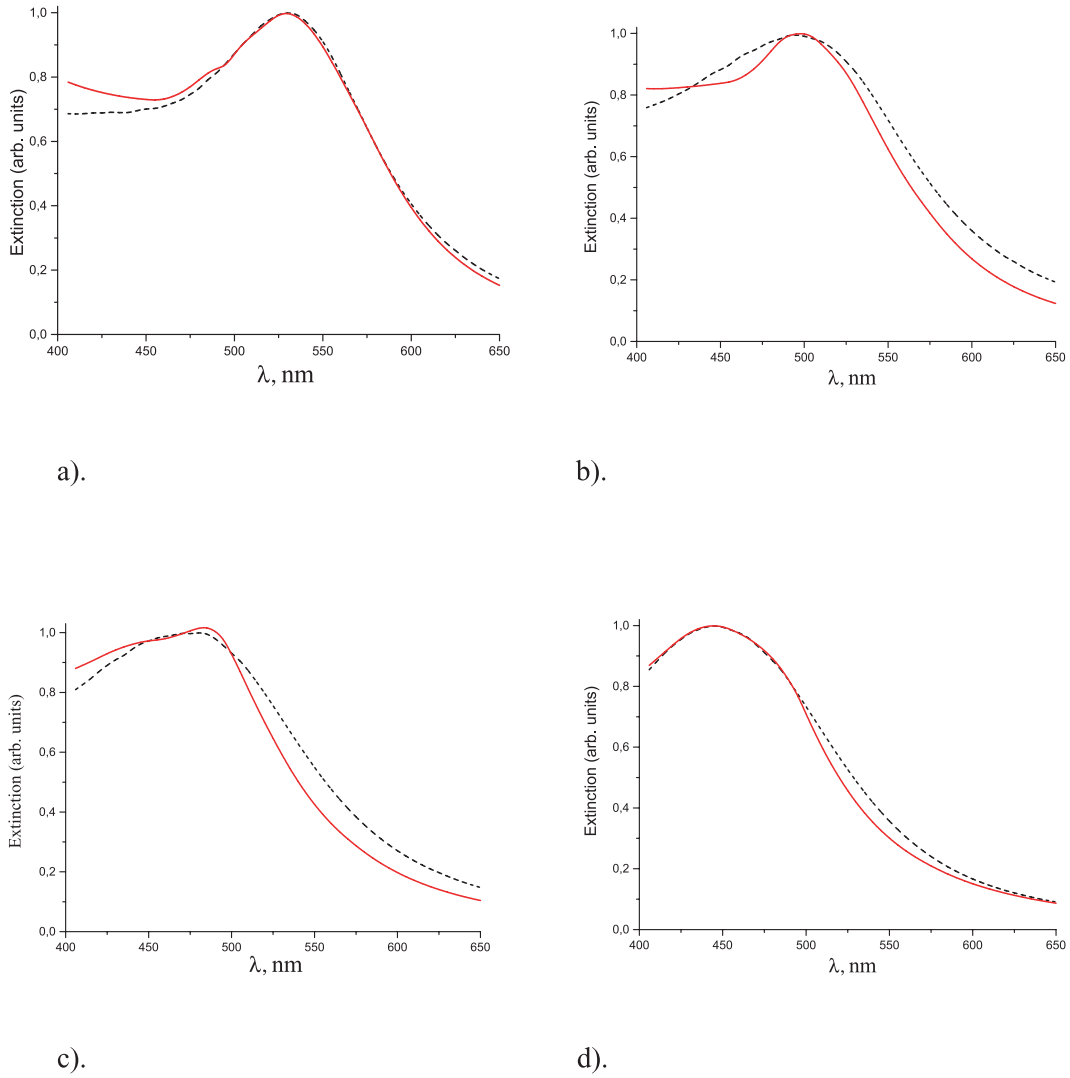

Fig. 3. Comparison of the experimental data (solid line) and simulated spectra (dotted line) for different gold relative content x: (a) $\alpha = 1$; (b) $\alpha = 0.66$ (c) $\alpha = 0.4$ (d) $\alpha = 0.3$.

nanoclusters had e.g. ellipsoidal shapes, then the spectra would be characterized by three distinct peaks of approximately equal magnitude, which was not found in experiments.

Thus, in general, the correspondence of experimental results and modeled spectra seems to be satisfactory and some important information about alloyed systems can be inferred from it. The most important problem that arises while nanoparticles formation is the determination of the metals relative concentrations inside the particle. This information can be obtained from the position of the absorption maximum. Figure 4 shows three curves for the peak wavelength position of the absorption spectrum versus the relative composition of gold (a) calculated by the conventional formula (11), (b) found from the advanced formula (12), and (c) found directly from the Mie theory based simulations.

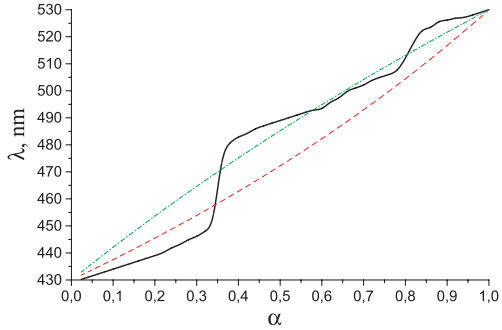

Fig. 4. Absorption peak versus gold relative content calculated by three different methods: (a) direct resonance maximum determination from the simulated absorption spectra (solid line); (b) with the use of equation (11) (dash line); (c) with the use of equation (12) (dot dash line).

It is evident that utilization of equation (11) for the determination of nanoparticles composition is not appropriate because its predictions deviate from the results obtained directly from the Mie simulations for the full range

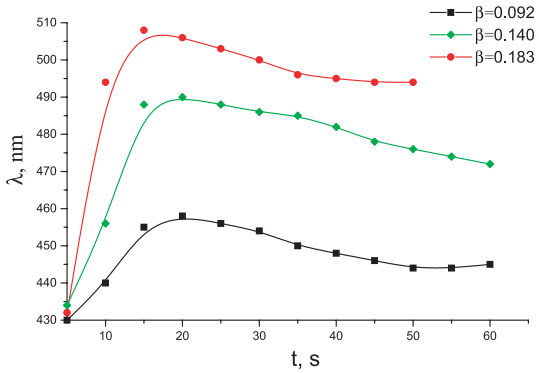

Fig. 5. Experimentally obtained absorption peak position versus time of the Ag/Au nanoparticles formation process for three different gold relative molar reactive mixture composition β: (1) $\beta = 0.092$; (2) $\beta = 0.140$; (3) $\beta = 0.183$.

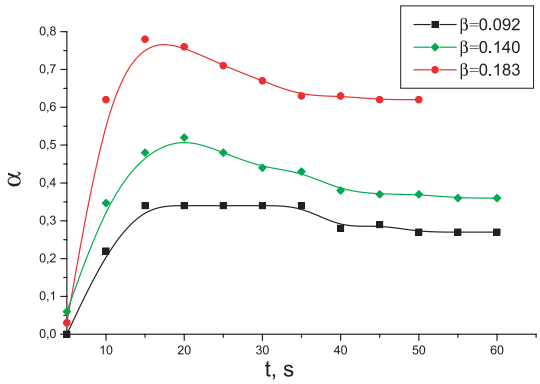

Fig. 6. Results of the calculation of the Ag/Au cluster composition temporal evolution for three different gold relative molar reactive mixture composition β: (1) $\beta = 0.092$; (2) $\beta = 0.140$; (3) $\beta = 0.183$.

of the gold concentrations and these deviations can lead to the mistakes of about 10% or even 20% which is not acceptable. On the contrary, results obtained from (12) show better correspondence to the Mie simulations, especially for the gold concentrations which are more than 0.4. This fact allows using the expression (12) for the preliminary estimation of the nanoparticles composition. However, the most exact way to find the composition is to perform full Mie theory based absorption spectra calculation and to establish correspondence between the composition and the peak wavelength position as it is presented by the solid line in Figure 4.

Described technique can be utilized to the on-line monitoring of the Ag/Au nanoparticles formation. Figure 5 represents the absorption peaks of the Ag/Au nanoparticles versus their formation time for different reactive mixture compositions. Figure 6 shows temporal evolution of the alloyed nanoparticles composition calculated with the use of the composition-resonance wavelength relation represented by the curve (c) in Figure 3. As it can be seen from Figure 6, the gold content in the clusters is zero at the beginning, then the cluster composition changes, gold amount increases and stabilizes on a constant value. Such composition time dependence is due to the differences in the two metallic phases nucleation rates (silver nucleates faster than gold). The phase separation process starts with the silver core formation and then co-precipitation of two metals follows according to a heterogeneous nucleation process. On the basis of the acquired information and assuming, for example, linear grows of the particle's size one can determine radial composition inside it. The latter is of prime importance for wide range of nanocomposites systems, especially for magnetic clusters, which magnetic properties depend strongly on the metallic phases distribution.

Optical properties of magnetic media in the UV-Vis-NIR range can be described again only in terms of dielectric function. Magnetic permeability for such frequency range remains to be almost unit even for ferromagnets [40]. But for the media with a spontaneous magnetization the dielectric function gets a tensorial form, with magnetization dependent non-diagonal elements. Though the letter demands a special expansion of the Mie theory for the anisotropic media, the situation with the magnetic media gets much simpler by taking into the consideration comparatively small values of the magnetooptical terms in the dielectric function. Consequently, the theoretical approach presented in this work remains valid and can be readily applied for the absorption spectra calculations. In the nearest future we are planning to advance into this direction and expand our theory to the case of the magnetic nanoparticles.

Proposed method for in situ monitoring of the alloyed nanoparticles composition is also very promising in the context of the design and creation of the modern optical filters tuned at the desired wavelength.

5 Conclusion

Polymer embedded alloyed nanoclusters systems are very promising multifunctional materials, that is why their investigation and elaboration of the new techniques for their formation and characterization are of prime importance. In this work Mie theory extension for the calculation of the absorption spectra of the alloyed nanoparticles composites have been considered in details. In the framework of the developed theoretical model the absorption spectra are calculated on the bases of the Mie theory for the single metal sphere, the dielectric function of which being dependent on the nanoparticle composition as the linear combination of the dielectric functions for the pure nanoparticulate metals. Calculated absorption spectra for the Ag/Au clusters showed good agreement with the experimental data.

The Au-Ag alloyed nanoparticles can be passivated by thiol and separated from the hydrophilic medium by centrifugation. These nanoparticles after purification can be dispersed in a polymer solution (e.g., polystyrene/chloroform) and high quality nanocomposite limiters obtained by spin-coating technology.

The primary attention was concentrated to the possibilities of the alloyed nanoclusters composition determination from the position of the absorption peaks. It was

shown that the most precise data can be obtained directly from the Mie theory spectra modeling. As an example, absorption peak versus relative gold content was calculated for the Ag/Au nanoclusters. At the same time, experimental data for the plasmonic resonance maximum behavior during nanoparticles formation was measured. With the use of these data it became possible to investigate temporal evolution of the Ag/Au nanoparticles relative content and even their radial composition.

It is worth noticing that suggested technique is by no means constrained by the Ag/Au systems. It can be readily used to the similar investigations for other bimetallic nanoclusters. The special interest lies in the area of the magnetic alloyed particles which can perform a unique magnetic properties at some appropriate compositions.

References

1. S.W. Han, Y. Kim, K. Kim, J. Colloid Interface Sci. **208**, 272 (1998)
2. D-H. Chen, C-J. Chen, J. Mater. Chem. **12**, 1557 (2002)
3. R.K. Roy, S.K. Mandal, A.K. Pal, Eur. Phys. J. B **33**, 109 (2003)
4. Y. Wang, N. Toshima, J. Phys. Chem. B **101**, 5301 (1997)
5. B. Bian, Y. Hirotsu, K. Sato, A. Makino, J. Electron Microsc. **48**, 753 (1999)
6. T. Liu, H. Shao, X. Li, J. Phys.: Condens. Matter **15**, 2507 (2003)
7. Koper O., I. Lagadic, K. J. Klabunde, Chem. Mater. **9**, 838 (1997)
8. T. Boronina, K. J. Klabunde, G.l Sergeev, Environ. Sci. Tech. **30**, 3645 (1996)
9. H. Bönnemann, W. Brijoux, R. Brinkmann, N. Matoussevitch, N. Waldöfner, Magnetohydrodynamics **39**, 29 (2003)
10. W. Eberhardt, Sur. Sci. **500**, 242 (2002)
11. R.G. Freeman, M.B. Hommer, K.C. Grabar, M.A. Jackson, M.J. Natan, J. Phys. Chem. **100**, 718 (1996)
12. S. Link, Z.L. Wang, M.A. El-Sayed, J. Phys. Chem B **103**, 3529 (1999)
13. P. Mulvaney, Langmuir **12**, 788 (1996)
14. A.G. de Leon, Y. Dirix, Y. Staedler, K. Feldman, G. Hhner, W. R. Caseri, P. Smith, Appl. Opt. **39**, 4847 (2001)
15. A.H. Lu, G.H. Lu, A.M. Kessinger, C.A. Foss, Jr., J. Phys. Chem B **101**, 9139 (1997)
16. R.D. Harris, J.S. Wilkinson, Sensors and Actuators B **29**, 261 (1995)
17. P. Mulvaney, M. Giersig, A. Henglein, J. Phys. Chem. **97**, 7061 (1993)
18. T. Yonezawa, N. Toshima, J. Chem. Soc. Faraday Trans. **91**, 4111 (1995)
19. S. Remita, M. Mostafavi, M.O. Delcourt, Radiat. Phys. Chem. **47**, 275 (1996)
20. L.M. Liz-Marzan, A.P. Philipse, J. Phys. Chem. **99**, 15120 (1995)
21. G.C. Papavassiliou, J. Phys. F: Met. Phys. **6**, L103 (1976)
22. Y. Mizukoshi, K. Okitsu, Y. Maeda, T.A. Yamamoto, R. Oshima, Y. Nagata, J. Phys. Chem. B **101**, 7033 (1997)
23. W. Caseri, Macromol. Rapid Commun. **21**, 705 (2000)
24. G. Carotenuto, B. Martorana, P. Perlo, L. Nicolais, in *Proceedings of the IEEE-nano 2004 August 17-19 2004, Munich, Germany, 2004, p. 207*
25. R. Salvati, A. Longo, G. Carotenuto, L. Nicolais, S. De Nicola, G.P. Pepe, Eur. Phys. J. B **41**, 43 (2004)
26. U. Kreibig, M. Vollmer, *Optical properties of metal clusters* (Springer, 1993)
27. C.F. Bohren, D.F. Huffman, *Absorption and Scattering of Light by Small Particles* (John Wiley & Sons, New York, 1983)
28. A. Liebsch, Phys. Rev. B **48**, 11317 (1993)
29. A. Pinchuk, G. Plessen, U. Kreibig, J. Phys. D: Appl. Phys. **37**, 3133 (2004)
30. G. Mie, Ann. Phys. **25**, 377 (1908)
31. L. Genzel, T. Martin, Phys. Status Solidi B **51**, 91 (1972)
32. Marcos M. Alvarez, Joseph T. Khoury, T. Gregory Schaaff, M.N. Shafigullin, I. Vezmar, R.L. Whetten, J. Phys. Chem. B **101**, 3706 (1997)
33. C.V. Fragstein, U.Z. Kreibig, Z. Phys. **224**, 306 (1969)
34. C.G. Granqvist, O. Hundery, Phys. Rev. B **16**, 3513 (1977)
35. A. Kawabata Kubo, R. J. Phys. Soc. Jpn. **21**, 1765 (1966)
36. M. Quinten, Z. Phys. B **101**, 211 (1996)
37. P. B. Johnson , R.W. Christy, Phys. Rev. B **6**, 4370 (1972)
38. K. Baba, T. Okuno, M. Miyagi, J. Opt. Soc. Am. B **12**, 2372 (1995)
39. A.M. Awwad, A.H. Al-Dujaili, H.E. Salman, J. Chem. Eng. Data **47**, 421 (2002)
40. A. Zvezdin, V. Kotov, *Modern Magnetooptics and Magnetooptical Materials* (IOP Publishing, Bristol and Philadelphia, 1997) 363 pp.